# Improving the Photoelectrochemical Performance of Nanostructured $TiO_2$ Films by Adsorption of Gold Nanoparticles†

**Nirmala Chandrasekharan and Prashant V. Kamat***

*Notre Dame Radiation Laboratory, Notre Dame, Indiana 46556-0579*

*Received: March 15, 2000*

$TiO_2$ films cast on conducting glass plates were modified by adsorbing gold nanoparticles (5 nm diameter) from a toluene solution. Selective formation of Au islands and larger particles on the $TiO_2$ surface could be seen from transmission electron micrographs and AFM images. Although the adsorbed Au particles are larger in diameter (50−70 nm), they retain surface plasmon characteristics, similar to those observed for smaller gold nanoparticles in solutions. A 3-fold enhancement in photocurrent generation has been achieved upon modification of $TiO_2$ films with Au nanoparticles. This improved photoelectrochemical performance is explained on the basis of improved interfacial charge-transfer kinetics of the $TiO_2$/Au composite film. Such semiconductor−metal composite films have potential applications in improving the performance of photoelectrochemical solar cells.

## Introduction

Nanostructured semiconductor films have been successfully employed as photoanodes in photoelectrochemical cells. The photoinduced charge separation achieved using the band gap excitation of the semiconductor films is crucial in maximizing the photocurrent generation efficiency. A variety of approaches have been considered by different research groups to maximize the charge separation in such films. One such approach involves the use of composite semiconductor nanoclusters.[1−4] By coupling two different semiconductor materials (i.e., sequential deposition of metal oxide and metal chalcogenide films on a conducting glass plate) it is possible to promote charge separation by accumulating electrons and holes in two different semiconductor layers.[5−7] For example, excitation of ZnO/CdS electrodes leads to the accumulation of electrons in the ZnO layer while the holes migrate to CdS and participate in the interfacial charge-transfer process.[5] The electrons are then efficiently transported to the collecting surface with minimal charge recombination. The concept of using such composite semiconductor films in dye-sensitized photochemical solar cells and in photocatalysis has been demonstrated in our earlier studies.[8,9]

Photoinduced deposition of noble metals such as Pt or Au on semiconductor nanoclusters has often been employed to enhance their photocatalytic activity.[10−12] For example, deposition of a noble metal on semiconductor nanoparticles is an essential factor for maximizing the efficiency of photocatalytic water splitting reactions. The noble metal (e.g., Pt), which acts as a sink for photoinduced charge carriers, promotes interfacial charge-transfer processes. A direct correlation between the work function of the metal and the photocatalytic activity for the generation of $NH_3$ from azide ions has been made for metallized $TiO_2$ systems.[13] In a recent picosecond laser flash photolysis study we showed that photogenerated electrons within the CdS nanoparticles migrate to the gold core within the laser pulse duration of 20 ps.[14] Both chemical and photodeposition are widely accepted methods for depositing noble metals on semiconductor nanoparticles. Recently, efforts have been made to bind metal nanoclusters to electrode surfaces using a self-assembled monolayer approach.[15−17] To the best of our knowledge, no significant effort has been made to investigate the effect of metal deposits on the photoelectrochemical properties of nanostructured semiconductor films. Such semiconductor−metal composite films can play an important role in improving the performance of photoelectrochemical cells (Scheme 1).

The deposition of platinum on short band gap semiconductors such as n-Si and n-GaAs has been shown to prevent the corrosion of electrodes in photoelectrochemical cells. While investigating the effect of metal deposition on the photoelectrochemical properties, Nakato and Tsubumora observed unusually high open-circuit voltages for n-Si electrodes.[18,19] On the other hand, gold film deposition on single-crystal $TiO_2$ electrodes led to a decrease in the photopotential.[20,21] This phenomenon was explained on the basis of a decreased bending of the conduction and valence bands. Recently, the size-dependent barrier height of nanosized Schottky contacts was evaluated using spatially resolved photocurrent measurements of copper-modified semiconductor surfaces.[22] An unusual photoelectrochemical effect has also been reported for Ni/$TiO_2$ nanocomposite films.[23] Carrier transit to the semiconductor/liquid interface was modulated by controlling the microenvironment within nanocomposite photoelectrodes. We report here photoelectrochemical properties of $TiO_2$/Au nanostructured composite films that were obtained by adsorbing gold nanoparticles from a toluene solution.

## Experimental Section

**Materials and Methods**. Titanium isopropoxide, 2-propanol, acetic acid, hydrogen tetrachloroaurate(III), toluene, tetraoctylammonium bromide, and sodium borohydride were purchased from Aldrich Chemical Co. and used without further purifica-

† Part of the special issue "Thomas Spiro Festschrift".

* Author to whom correspondence should be addressed. E-mail: pkamat@nd.edu;http://www.nd.edu/~pkamat.

10.1021/jp0010029 CCC: $19.00 
Published on Web 09/07/2000

**SCHEME 1: Charge Separation in a Gold-Nanoparticle-Modified Nanostructured $TiO_2$ Electrode**

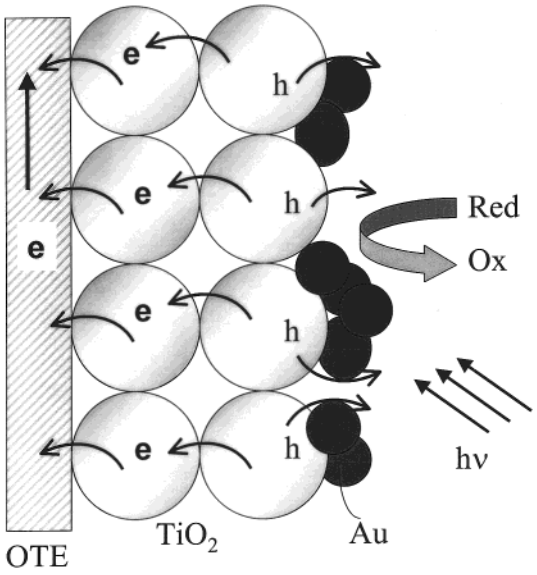


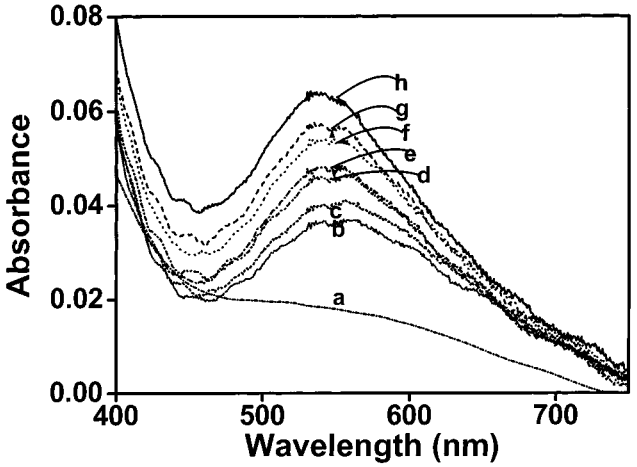


**Figure 1.** Absorbance spectra of the $TiO_2$ film during the adsorption of Au nanoparticles. The spectra were recorded following the immersion of OTE/$TiO_2$ electrode in the colloidal gold solution in toluene at time intervals: $a = 0$, $b = 15$, $c = 30$, $d = 45$, $e = 90$, $f = 120$, $g = 180$, and $h = 240$ min.

tion. Optically transparent electrodes (OTE) were cut from a transparent electrically conducting glass sheet (TEC Glass) obtained from Pilkington (Libbey Owens Ford). Atomic force microscopy (AFM) was carried out using a digital nanoscope (Nanoscope IIIa) in the tapping mode. An etched silicon tip was used as a probe for imaging the $TiO_2$ and Au/$TiO_2$ surface. Absorption spectra were recorded using a Shimadzu 3101 spectrometer. A Hitachi S-4500 scanning electron microscope (SEM) was employed to record the images of the nanostructured semiconductor films with either 150 or 200 K magnifications. The films were cast on conducting glass substrates (1 $cm^2$) using the procedure described above.

**Synthesis of $TiO_2$ and Au−$TiO_2$ Electrodes.** Colloidal $TiO_2$ was prepared by the hydrolysis of titanium isopropoxide in acetic acid medium (0.6 M) and autoclaving the sol at 500 K. Roughly 100 $\mu$L of the $TiO_2$ suspension was applied to the OTE glass substrate by syringing the solution onto the electrode and allowing it to dry at room temperature. The OTE electrodes coated with $TiO_2$ film (Area 2.5 $cm^2$, ~10 $\mu$m thick) were then heated to 673 K for 1 h.

The $TiO_2$ films were modified with gold nanoparticles by immersing the electrodes in a toluene solution containing 9 mM of Au colloid. Synthesis of stable and organically solubilized gold nanoparticles using a phase transfer catalyst are described elsewhere.[24,25] Usually the $TiO_2$ electrode was kept in contact with the gold colloid suspension overnight (10−12 h) to maximize the adsorption of gold colloids.

**Electrochemical and Photoelectrochemical Measurements.** The measurements were carried out in a quartz cell with two side arms attached for inserting reference (SCE) and counter (Pt gauze) electrodes. The electrolyte was 0.05 M NaOH. In the experiment involving pH variation, $NaClO_4$ was used as the neutral solution and NaOH or $HClO_4$ was added in appropriate amounts to vary the pH. The illumination of the electrode was from the substrate side (front face illumination) in all the measurements. I−V characteristics were recorded using Princeton Applied Research, model 175 galvanostat/potentiostat. Photocurrent measurements were carried out using a Keithley model 617 programmable electrometer. A collimated light beam from a 150 W xenon lamp was used for UV illumination. A Bausch and Lomb high-intensity grating monochromator was introduced into the path of the excitation beam for selecting the wavelengths.

## Results and Discussion

**Absorption Spectra of Au-Modified $TiO_2$ Electrode.** The absorption spectra of the $TiO_2$ electrode recorded following the adsorption of gold colloids are shown in Figure 1. The spectra recorded (following the immersion of electrode in colloidal gold solution) at different times show a prominent absorption band in the visible with a maximum at 546 nm. The growth of this band with increasing immersion time of the $TiO_2$ electrode confirms the adsorption of gold colloids onto the $TiO_2$ surface. This absorption band at 546 nm is characteristic of the surface plasmon band of gold nanoparticles and arises as a result of the collective modes of oscillation of the free conduction band electrons induced by an interacting electromagnetic field. This plasmon absorption is red-shifted compared to the solution spectra of gold colloids and is attributed to the surrounding $TiO_2$ medium. Interfacial as well as interparticle interactions dictate the shift and broadening of the plasmon band of the Au particles adsorbed on $TiO_2$ films. The dependence of the spectral shift of the plasmon band on the dielectric constant of the embedding medium has been studied by Kreibig and co-workers.[26,27] These researchers observed a strong red-shift in the plasmon band of Ag nanoclusters when they were embedded in a $SiO_2$ or $TiO_2$ matrix. The dependence of the shift on the chemically differing embedding medium indicates the high sensitivity of surface plasmon band to cluster−matrix interface properties.

**AFM and Electron Micrographs.** The AFM image (top view) of an Au−$TiO_2$ film is shown in Figure 2. The image was recorded in the tapping mode using an etched silicon tip. The blank $TiO_2$ films consist of fairly uniform size particles of diameter 30−40 nm. As can be seen from Figure 2, smaller $TiO_2$ particles lie in the background of the AFM image while slightly bigger size gold particles lie close to the tip. The clustering of gold nanoparticles at selective $TiO_2$ sites, which were seen in AFM images, could not be resolved further.

To assess the morphology of the Au−$TiO_2$ film, we obtained scanning electron micrographs of the $TiO_2$ (Figure 3A) and Au−$TiO_2$ films (Figure 3B,C). These two pictures show two distinct types of gold nanoparticle adsorption on $TiO_2$ films. In Figure

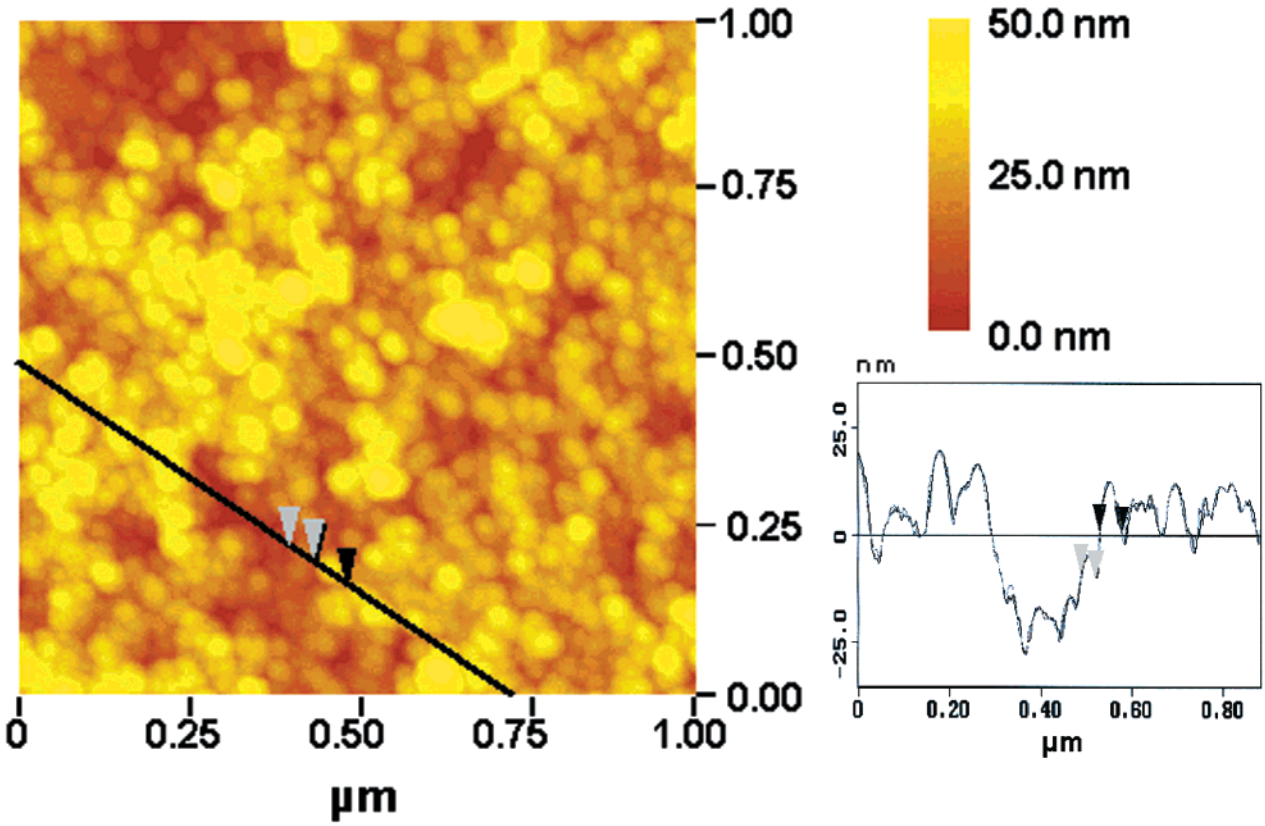


**Figure 2.** Atomic force microscopy of $TiO_2$ nanostructured film modified with gold nanoparticles. The cross-section view shows the presence of larger gold particles (50−70 nm) at the surface.

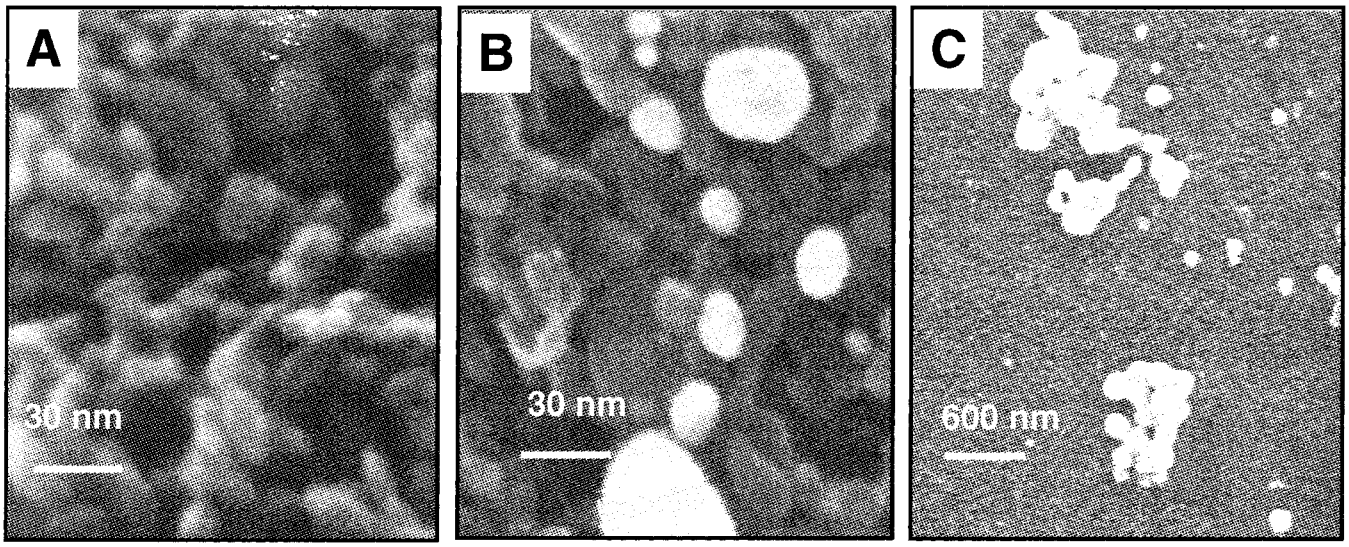


**Figure 3.** Scanning electron micrographs of nanostructured $TiO_2$ films cast on a conducting glass substrate: (a) before modification, and (b and c) following the adsorption of Au nanoparticles from a toluene solution.

3B we observe well-separated gold nanoparticles with a diameter in the range of 20−70 nm. These particles also have a tendency to aggregate and exist as islands of gold nanoclusters on the $TiO_2$ surface (Figure 3C). It is evident from these pictures that the gold nanoparticles grow in size as they get adsorbed onto the $TiO_2$ film. The gold nanoparticles prepared in toluene have particle diameters of ∼5 nm. Capping of the gold nanoparticles by tetraoctylammonium bromide (phase transfer catalyst) keeps these particles stable in toluene solution with no apparent growth in the particle size. The larger particle size of gold nanoparticles seen in AFM and SEM images indicates that the gold nanoparticles aggregate/coalesce and grow in size during the adsorption process. Formation of cluster islands is also an indication that these particles prefer selective sites for adsorption on the $TiO_2$ surface. Despite this clustering effect, the adsorbed gold nanoparticles retain their individual character as they exhibit the characteristic plasmon absorption band in the visible.

**Photoresponse of OTE/$TiO_2$/Au Electrodes.** The photocurrent action spectra of OTE/$TiO_2$ electrodes before and after modification by Au colloids are shown in Figure 4. The incident photon to current conversion efficiency (IPCE) defined as the number of electrons collected per incident photon, was evaluated

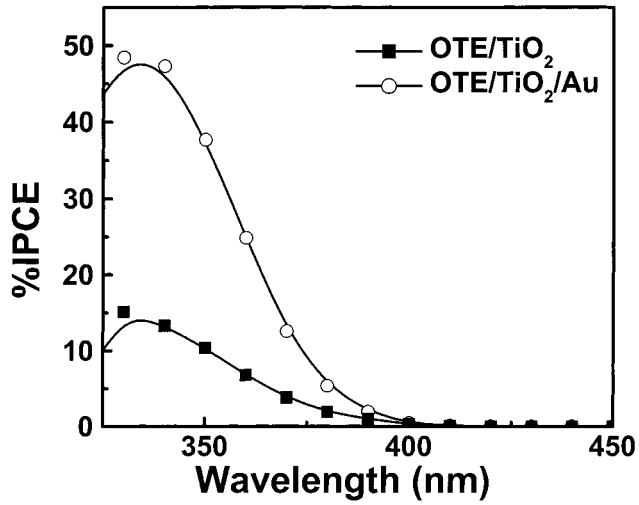


**Figure 4.** Photocurrent action spectra of OTE/$TiO_2$ and OTE/$TiO_2$/Au electrodes in 0.05 M NaOH. The incident photon to charge carrier generation efficiency (IPCE) was determined by recording photocurrent at different excitation wavelengths and using expression (1).

from short circuit photocurrent ($I_{sc}$) measurements at different wavelengths ($\lambda$) and using the following expression (eq 1):

$$\text{IPCE\%} = [1240 \times I_{sc}\,(\text{A/cm}^2)]/[\lambda\,(\text{nm}) \times I_{inc}(\text{W/cm}^2)] \times 100 \quad (1)$$

where $I_{inc}$ is the incident light power. Both OTE/$TiO_2$ and OTE/$TiO_2$/Au electrodes show photocurrent generation at wavelengths below 410 nm. Both these electrodes exhibit similar onset wavelengths for photocurrent generation that correspond to the band gap excitation of $TiO_2$ ($E_g = 3.2$ eV). Thus, adsorbed gold nanoparticles do not exhibit any noticeable influence on the spectral response of the OTE/$TiO_2$/Au electrodes. However, a significant (nearly 3-fold) enhancement in the magnitude of photocurrent is seen, upon adsorption of gold nanoparticles on the $TiO_2$ electrodes. The maximum IPCE observed for OTE/$TiO_2$/Au electrode at 320 nm is around 50%. The 3-fold enhancement in the photocurrent generation efficiency is indicative of the fact that the adsorption of Au nanoparticles is beneficial for promoting the charge separation within the nanostructured $TiO_2$ network as well as improving the interfacial charge-transfer processes. Blank experiments carried out with OTE/$TiO_2$ electrodes pretreated with a toluene solution of tetraoctylammonium bromide had no effect on the photoelectrochemical performance of $TiO_2$ films.

**I−V Characteristics.** The dependence of photocurrent on the applied potential provides important information concerning the photoelectrochemical behavior of nanostructured semiconductor films. The dependence of the photocurrent as a function of applied potential for OTE/$TiO_2$ and OTE/$TiO_2$/Au are shown in Figure 5. At positive potentials a steady flow of current is seen during the illumination of both these electrodes. The observed photocurrent is nearly 4-fold larger for the $TiO_2$ electrodes modified with gold nanoparticles under positive bias. The photocurrent time profiles recorded at 0.75 and −0.95 V vs SCE are shown in Figure 6, parts A and B, respectively. The photocurrent generation was prompt and the current was stable in the time interval of the pulsed illumination. The OTE/$TiO_2$/Au electrode shows higher photocurrent than OTE/$TiO_2$ at both these extreme bias potentials. While the photocurrent generation is steady at +0.75 V, a small decay of the photocurrent was noticeable at −0.95 V vs SCE. Since this

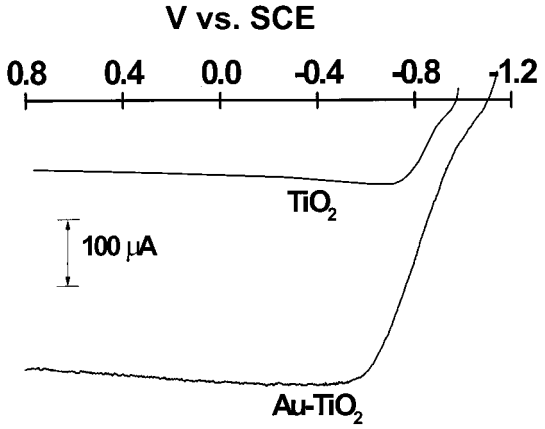


**Figure 5.** The dependence of the photocurrent as a function of applied voltage under UV irradiation ($\lambda$ > 300 nm). (Electrolyte 0.05 M NaOH, CE: Pt and RE: SCE).

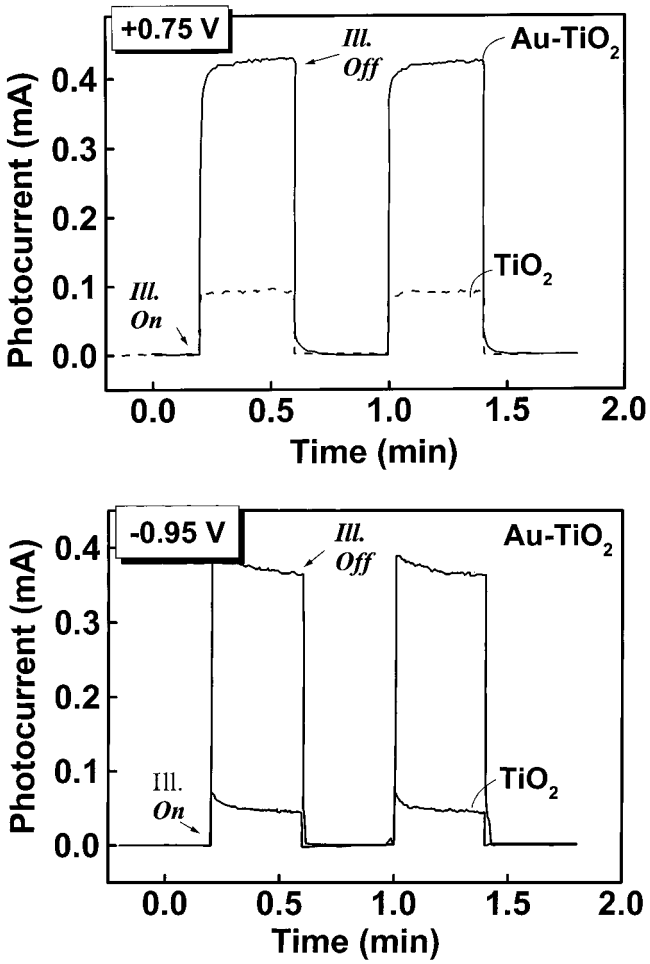


**Figure 6.** The photocurrent response of the OTE/$TiO_2$ and OTE/$TiO_2$/Au electrodes to UV irradiation. The electrodes were maintained at (A) +0.75 V and (B) −0.95 V vs SCE. (Electrolyte: $N_2$-saturated 0.05 M NaOH, CE: Pt and RE: SCE).

potential is close to the zero current potential of $TiO_2$, we expect a minimal driving force for the collection of photogenerated electrons at the OTE surface. It is interesting to note however, that the OTE/$TiO_2$/Au electrode yields significantly higher photocurrent at this negative bias.

An interesting observation in these experiments is the effect of Au nanoparticle deposition on the zero current potential of the $TiO_2$ electrode. At this potential the driving force required

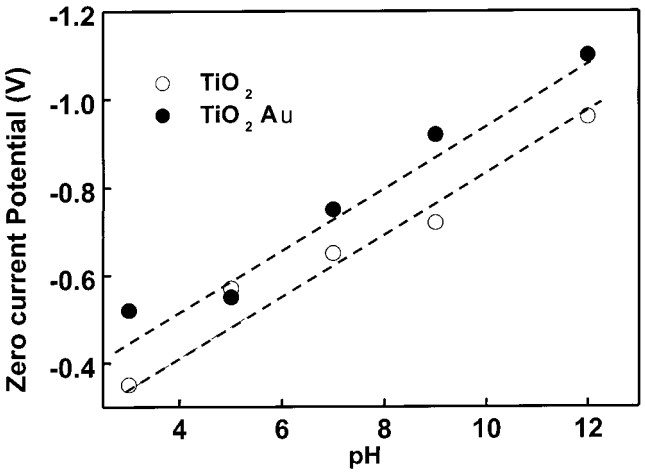


**Figure 7.** pH dependence of the zero current potential ($V_{i=0}$) of OTE/$TiO_2$ and OTE/$TiO_2$/Au electrodes. $V_{i=0}$ was measured from the zero current potential in the I−V plot recorded under UV illumination. The counter electrode and reference electrodes were Pt and SCE, respectively. The pH of the electrolyte containing 0.05 M $NaClO_4$ was adjusted using NaOH or $HClO_4$.

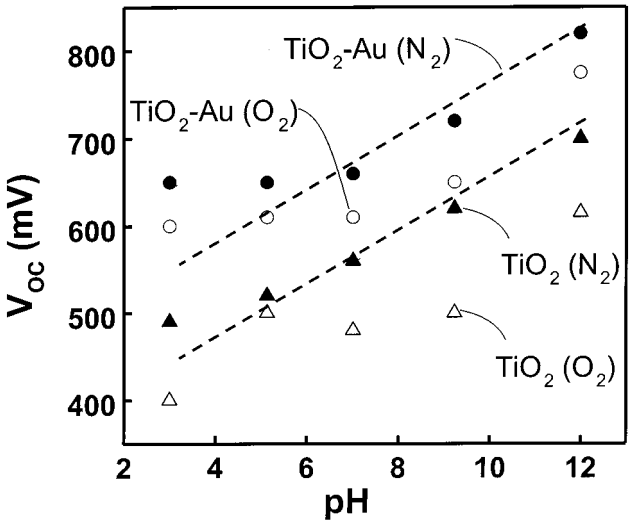


**Figure 8.** Dependence of the open-circuit potential on the medium pH following UV illumination of OTE/$TiO_2$ and OTE/$TiO_2$/Au electrodes. (Electrolyte 0.05 M $NaClO_4$, ($N_2$-saturated), CE: Pt).

to transport the electrons across the particulate film diminishes and all the photogenerated charges are lost in the recombination process. For a single-crystal semiconductor electrode, such a zero current potential represents the flat band potential. However, for a nanostructured semiconductor film electrode, this value can be regarded as an apparent flat band potential since the kinetic factors control the net flow of electrons. From Figure 5 one can infer that this zero current potential of $TiO_2$ shifts from −0.98 to −1.13 V upon modification with gold nanoparticles. Such a negative shift (∼150 mV) in the zero current potential shows the ability of the $TiO_2$/Au composite films to suppress the charge recombination by facilitating hole transfer to the redox couple in the electrolyte.

We further evaluated the dependence of the zero current potential on the solution pH. The band energies of metal oxide semiconductors such as $TiO_2$ show strong pH dependence. Because of the surface protonation/deprotonation equilibria, the band energies shift 0.059 V per pH unit. For the bulk $TiO_2$ semiconductor, the dependence of the flat band potential ($E_{fb}$) on the solution pH obeys expression 2:

$$E_{fb} = E_0 - 0.059\ \mathrm{pH} \qquad (2)$$

Although an exact estimate of flat band potential for nanostructured $TiO_2$ film is rather difficult, one can monitor zero current potential, which qualitatively represents apparent flat band potential of the $TiO_2$ film. We monitored the zero current potential of OTE/$TiO_2$/Au by recording I−V characteristics at different pH. The zero current potential (or apparent flat band potential) became more negative with increasing pH of the medium (Figure 7). The dotted line is a fit based on expression (2) and using the value of $E_0$ as −0.2 V (V vs SCE). For the Au−$TiO_2$ electrode a parallel trend was observed for the entire pH range, but with a 150 mV shift. This again confirms that the kinetic factors responsible for the shift in the zero current potential prevail over a wide pH -range.

**Influence of pH on the Open-Circuit Voltage.** Although the photoelectrochemical behavior of nanostructured semiconductor film deviates from the conventional single-crystal electrode, the generation of photovoltage is directly dependent on the electron accumulation following band gap excitation. As shown earlier, the scavenging of one of the charge carriers (viz., holes for the n-type semiconductor films) at the semiconductor−electrolyte interface dictates the magnitude of the photovoltage generation.[28−30]

In the dark, the Fermi level equilibrates with the redox couple present in the electrolyte. Upon excitation of $TiO_2$ films, one observes a rise in the photovoltage as the holes are scavenged by the $OH^-$ at the interface, while electrons accumulate within the particles. As the electrons accumulate in the $TiO_2$ particulate film, the pseudo-Fermi level ($E'_F$) shifts, thus, attaining a new photoequilibrium. For an intrinsic semiconductor we can express $E'_F$ by expression (3):[31]

$$E'_F = E_{CB} + kT \ln(n_c/N_c) \qquad (3)$$

where $E_{CB}$ is conduction band energy, $N_c$ is the effective state density and $n_c$ is the carrier density including the accumulated electrons. Any shift in $E'_F$ thus represents increased accumulation of electrons in the $TiO_2$ particulate film.

The magnitude of the photovoltage ($V_{OC}$) represents the energy difference ($\Delta E$) between the apparent Fermi level of the $TiO_2$ film and the reduction potential of the redox couple in the electrolyte (4):

$$\Delta E = E'_F - E^0_{redox} \qquad (4)$$

We monitored the open-circuit potential of OTE/$TiO_2$ and OTE/$TiO_2$/Au at different pH (Figure 8). $V_{OC}$ increases with increasing pH as the conduction band shifts to more negative potentials. The OTE/$TiO_2$/Au electrodes consistently yielded higher $V_{OC}$ (∼150 mV) than the OTE/$TiO_2$ electrode, but maintains a similar slope. These observations again confirm the fact that the adsorbed Au nanoparticles improve the accumulation of electrons within the $TiO_2$ particulate film by facilitating the hole transfer at the electrolyte interface. The slope of the plot in Figure 8 (∼30 mV) is lower than the 59 mV/pH expected from the ideal photoelectrochemical behavior of a semiconductor electrode. The lack of space charge layer and the susceptibility of nanostructured semiconductor films to charge recombination at the grain boundaries affect the net photopotential. Moreover, the adsorbed species can also affect the electron acumulation process. For example the photopotential at a nanostructured $TiO_2$

film is extremely sensitive to dissolved oxygen as the electrons are scavenged at the electrolyte interface. Upon purging the electrolyte with oxygen, the photopotential decreased as the dissolved oxygen scavenged the photogenerated electrons (Figure 8). The role of oxygen on the photoelectrochemical behavior of $TiO_2$ electrodes is discussed elsewhere.[4,32]

Altered energetics of the $TiO_2$/Au composite may also be considered as an alternate possibility for explaining the increase in the photovoltage. When semiconductors such as $TiO_2$ are in contact with a metal such as gold, the Fermi level equilibration shifts the flat band potential of the semiconductor to more positive potentials. (The Fermi level of bulk gold is around +0.5 V vs NHE.) As a result of such a shift in energy, one expects a decrease in the photovoltage as has been noted in the case of single-crystal $TiO_2$ electrode that was deposited with thin Pt film.[20,21] But when the deposited metal film is in the form of small islands or in nanoparticulate form an enhancement in the photovoltage is possible.[19] The metal nanoparticles are considered to be highly electronegative because of the shift in the Fermi level to negative potentials.[33] This shift can be more dramatic when metal nanoparticles are surrounded by electron donors.[33,34] Although we cannot totally rule out such an altered energetic argument for the $TiO_2$/Au composite film, we consider this effect to be small. First of all, the adsorption of the gold particles is very small and is limited only to the outer layer of $TiO_2$. Second, net electron accumulation within the $TiO_2$ particles controls the Fermi level of the $TiO_2$ film, thus, overriding any effects introduced by Fermi level equilibration. This aspect is also supported by the fact that the photocurrent generation in nanostructured film is controlled by kinetic factors and not by the electric field effects.[35,36]

An important factor for achieving higher IPCE is the improved interfacial charge transfer at the OTE/$TiO_2$/Au electrode−electrolyte interface. The adsorbed gold nanoparticles are expected to decrease the overvoltage that is necessary for the hole transfer to the redox couple in the electrolyte. The improved photoconversion efficiency in Figure 4 confirms this argument. It may be noted that the influence of decreased overvoltage on the interfacial charge-transfer process has also been demonstrated earlier, in semiconductor particle-assisted photocatalytic reactions[13] and p-GaAs single-crystal-based photoelectrochemical cells.[37] By promoting the interfacial hole transfer to the redox couple, the adsorbed gold nanoparticles facilitate charge (electron) stabilization within the nanostructured $TiO_2$ films. Thus, the electrons can be transported to the collecting surface of OTE with minimal encounter of charge recombination losses. Effort has also been made to improve the photocurrent generation of semiconductor film electrodes by preparing Ni/$TiO_2$ nanocomposite films. An improved efficiency for hole transfer was achieved by chemically modifying these films with nickel ferrocyanate centers. Variation in flat band potential as well as changes in the recombination rates have been investigated for the metal-modified semiconductor surfaces. Locally measured photocurrent/voltage measurements confirmed size-dependent barrier heights for the nanometal−semiconductor contacts.[22]

## Conclusions

Maximizing the charge separation efficiency in a nanostructured semiconductor film has often been the major goal for improving the performance of photoelectrochemical cells. A common approach for achieving this goal is to employ redox couples that efficiently scavenge the photogenerated holes at the semiconductor/electrolyte interface. While such redox couples are to some degree useful in achieving charge separation in nanostructured semiconductor films, they do not completely overcome the effects of charge recombination. The present study shows that semiconductor−metal composite films are capable of achieving further improvements in the photoinduced charge separation and in the overall photoconversion efficiency. The adsorbed gold nanoparticles play an important role in maximizing the photocurrent generation and increasing the photovoltage by ~150 mV by improving the interfacial charge-transfer kinetics. The observed 3-fold enhancement in the photoconversion efficiency demonstrates the usefulness this approach for improving the photoconversion efficiency of dye-sensitized solar cells and photocatalytic reactions.

**Acknowledgment.** We thank Dr. K. George Thomas for helpful discussions and Dr. Frank Peres for his assistance in recording SEM pictures. The research described herein was supported by the Office of Basic Energy Science of the Department of the Energy. This is contribution NDRL 4213 from the Notre Dame Radiation Laboratory.

## References and Notes

(1) Gerischer, H.; Luebke, M. *J. Electroanal. Chem. Interfacial Electrochem.* **1986**, *204*, 225.

(2) Spanhel, L.; Weller, H.; Henglein, A. *J. Am. Chem. Soc.* **1987**, *109*, 6632.

(3) Gopidas, K. R.; Bohorquez, M.; Kamat, P. V. *J. Phys. Chem.* **1990**, *94*, 6435.

(4) Vinodgopal, K.; Bedja, I.; Kamat, P. V. *Chem. Mater.* **1996**, *8*, 2180.

(5) Hotchandani, S.; Kamat, P. V. *J. Phys. Chem.* **1992**, *96*, 6834.

(6) Vogel, R.; Hoyer, P.; Weller, H. *J. Phys. Chem.* **1994**, *98*, 3183.

(7) Zaban, A.; Micic, O. I.; Gregg, B. A.; Nozik, A. J. *Langmuir* **1998**, *14*, 3153.

(8) Nasr, C.; Hotchandani, S.; Kim, W. Y.; Schmehl, R. H.; Kamat, P. V. *J. Phys. Chem. B* **1997**, *101*, 7480.

(9) Nasr, C.; Hotchandani, S.; Kamat, P. V. *J. Phys. Chem. B* **1998**, *102*, 10047.

(10) Heller, A. *Pure Appl. Chem.* **1986**, *58*, 1189.

(11) Heller, A. *NATO Asi Ser., Ser. C* **1986**, *15*.

(12) Domen, K.; Sakata, Y.; Kudo, A.; Maruya, K.; Onishi, T. *Bull. Chem. Soc. Jpn.* **1988**, *61*, 359.

(13) Nosaka, Y.; Norimatsu, K.; Miyama, H. *Chem. Phys. Lett.* **1984**, *106*, 128.

(14) Shanghavi, B.; Kamat, P. V. *J. Phys. Chem. B* **1997**, *101*, 7675.

(15) Amihood, D.; Katz, E.; Willner, I. *Langmuir* **1995**, *11*, 1313.

(16) Colvin, V. L.; Goldstein, A. N.; Alivisatos, A. P. *J. Am. Chem. Soc.* **1992**, *114*, 5221.

(17) Yonezawa, T.; Mutsune, H.; Kunitake, T. *Chem. Mater.* **1999**, *11*, 33.

(18) Nakato, Y.; Tsubomura, H. *J. Photochem.* **1985**, *29*, 257.

(19) Nakato, Y.; Ueda, K.; Yano, H.; Tsubomura, H. *J. Phys. Chem.* **1988**, *92*, 2316.

(20) Nakato, Y.; Tsubomura, H. *Isr. J. Chem.* **1982**, *22*, 180.

(21) Nakato, Y.; Shioji, M.; Tsubomura, H. *Chem. Phys. Lett.* **1982**, *90*, 453.

(22) Hiesgen, R.; Meissner, D. *J. Phys. Chem. B* **1998**, *102*, 6549.

(23) de Tacconi, N. R.; Carmona, J.; Rajeshwar, K. *J. Phys. Chem. B* **1997**, *100*, 10151.

(24) Fink, J.; Kiely, C.; Bethell, D.; Schiffrin, D. J. *Chem. Mater.* **1998**, *10*, 922.

(25) George Thomas, K.; Kamat, P. V. *J. Am. Chem. Soc.* **2000**, *122*, 2655.

(26) Kreibig, U.; Vollmer, M. *Optical Properties of Metal Clusters*; Springer: Berlin, 1995.

(27) Kreibig, U.; Gartz, M.; Hilger, A.; Hovel, H. Mie-plasmon spectroscopy: A tool of surface science. In *Fine Particles Science and Technology*; Pelizzatti, E., Ed.; Kluwer Academic Publishers: Boston, 1996; p 499.

(28) Hodes, G.; Howell, I. D. J.; Peter, L. M. *J. Electrochem. Soc.* **1992**, *139*, 3136.

(29) Hagfeldt, A.; Bjorksten, U.; Lindquist, S. E. *Sol. Energy Mater. Sol. Cells* **1992**, *27*, 293.

(30) Vinodgopal, K.; Hotchandani, S.; Kamat, P. V. *J. Phys. Chem*. **1993**, *97*, 9040.
(31) Myamlin, V. A.; Pleskov, Y. V. *Electrochemistry of semiconductors*; Plenum Press: New York, 1967.
(32) Vinodgopal, K.; Stafford, U.; Gray, K. A.; Kamat, P. V. *J. Phys. Chem*. **1994**, *98*, 6797.
(33) Henglein, A.; Holzwarth, A.; Mulvaney, P. *J. Phys. Chem*. **1992**, *96*, 8700.
(34) Linnert, T.; Mulvaney, P.; Henglein, A. *Ber. Bunsen-Ges. Phys. Chem*. **1991**, *95*, 838.
(35) Zaban, A.; Ferrere, S.; Gregg, B. A. *J. Phys. Chem. B* **1998**, *102*, 452.
(36) Cahen, D.; Hodes, G.; Graetzel, M.; Guillemoles, J. F.; Riess, I. *J. Phys. Chem*. **2000**, *104*, 2053.
(37) Meier, A.; Uhlendorf, I.; Meissner, D. *Electrochim Acta* **1995**, *40*, 1523.